Sumer Journal for Pure Science (ISSN: 2790-7031)
SJPS 2023 (December), Vol. 2, No. 2, p.p.: 157-172

The Influence of Various Impurities on the Electronic Properties of the n-Triangulene Graphene Nanoflakes

Tuqa A. Omeer [1] and Mohammed H. Mohammed [1,2,*]

[1]Department of Physics, College of Science, University of Thi-Qar, Nassiriya 64000, IRAQ.
[2]Department of Physics, College of Science, Southern Illinois University, Carbondale, IL62901 USA.

Abstract:

The electronic properties of the n-triangulene graphene nanoflakes (nT-GNFs) are investigated with and without various concentrations of (Si, P, Ge, and As) impurities in different locations via using DFT methods. Results showed very fascinating results. The 3T-GNFs, 4T-GNFs, 5T-GNFs, and 6T-GNFs have semiconductor behaviors. So, the electronic band gap is depended on the type and site of the impurity. By using the same locations of impurities in all structures, but with different impurity, the electronic band gap is altered. We detected that all structures became more stable and lower reactive with these impurities in different sites due to the total energy is increased. Also, some of these structures have weak interact with others structures. There are higher energy required to donating/accepting an electron to become cation/anion. In brief, the results shown the electronic properties of all structures depended on the type and location of the impurity. Then, we can use these impurities to enhancement the electronic properties of the nT-GNFs.

Keywords: DFT; nT-GNFs, various impurities-doped nT-GNFs; electronic band gap; total energy.

تأثير الشوائب المختلفة على الخصائص الإلكترونية لرقائق الكرافين وتراكيب مختلفة من التريانجولين النانوية

تقى علي عمير[1] ، محمد هلول محمد [*،1،2]

[1] قسم الفيزياء، كلية العلوم ، جامعة ذي قار ، ذي قار ، العراق
[2،] قسم الفيزياء، كلية العلوم، جامعة جنوب إلينوي، كاربوندیل، ، الولايات المتحدة الأمريكية.*

الخلاصة :

في هذه الدراسة ، تمت دراسة الخصائص الإلكترونية لرقائق الكرافين وتراكيب مختلفة من التريانجولين النانوية في الحالة النقية ومع تركيزات مختلفة من الشوائب (Si، P، Ge، As) وفي مواقع مختلفة باستخدام نظرية الكثافة الوظيفية. حيث أظهرت اضافة هذه الشوائب نتائج رائعة جدا". أوضحت النتائج ان التراكيب (3T-GNFs, 4T-GNFs, 5-TGNFs, and 6-TGNFs تسلك سلوك أشباه الموصلات. وان فجوه الطاقة تعتمد على موقع الشوائب وكذلك نوعها. وقد أبدت نفس النتائج عند استخدام نفس المواقع للشوائب في التراكيب المختلفة اعلاه. برهنت النتائج ان هذه الشوائب تزيد من استقراريه التراكيب حيث اصبحت التراكيب اكثر استقرارا" واقل تفاعلا" مع هذه الشوائب في مواقع مختلفة وذلك بسبب زيادة الطاقة الكلية. كما أن بعض هذه التراكيب لها تفاعل ضعيف مع تراكيب أخرى حيث ان هناك طاقة أعلى مطلوبة للتبرع/قبول الإلكترون ليصبح كاتيون/أنيون. وأكدت هذه الدراسة أن الخصائص الإلكترونية لجميع هذه التراكيب تعتمد على نوع وموقع الشوائب. وبذلك يمكننا استخدام هذه الشوائب لتعزيز الخصائص الإلكترونية لـتراكيب (nT-GNFs).

* mohammedph14@gmail.com

Graphene has recently been the subject of in-depth study by a number of academics due to its intriguing features and prospective applications [1-3]. For instance, graphene's strong carrier mobility, high saturation velocity, and long spin diffusion length have made it possible to create intriguing electronics and spintronics based on graphene. Graphene is not suited for transistor applications, however, because it lacks an energy band gap[3-8]. Graphene can be sliced into graphene nanoflakes as a way to make a finite band gap in it. However, the shapes, sizes, and environmental factors that affect graphene nanoflakes' behavior can be quite important [9]. It is critical to comprehend how these components affect the properties of graphene nanoflakes in order to take full advantage of graphene's enormous promise in electronics and spintronics [10].

The research community has shown a great deal of interest in the narrow graphene strips known as graphene nanoribbons, which are one of the numerous possible configurations of graphene nanoflakes. These strips are considered to be promising quasi-one-dimensional materials for electronic nanodevices [4, 11-13]. On the other hand, other graphene flakes might also be interesting investigating. The on-surface synthesis of triangulene, a molecule with two unpaired electrons, has just recently proven successful. To make triangle-shaped graphene nanoflakes that can be enlarged from triangulene, however, this unique method of chemical synthesis may be applied in the near future. Therefore, the focus of this study is on a series of triangle-shaped graphene nanoflakes [14].

In the present work, we will study various electronic properties of the nT-GNS (where n=3-6) with and without different impurities of (Si, P, Ge , and As) impurities in the different locations to develop the electronic properties of the nT-GFs. These properties are studied by utilizing DFT methods.

1. Computational details

In this study, DFT calculations that were implemented in the Gaussian 09 package [15, 16] with the basis set B3LYP/6-31G were used to optimize the structure of nT-GNFs [12, 15, 17-22]. We actually selected this basis set because it is adequate for related geometry optimizations of this molecule [21–25]. The relaxing of the molecular structures was the first step in our computation. After that, we looked at the molecules' electronic properties, including their electronic band gap (E_{gap}), total energy (E_T), and Fermi energy level (E_{Fl}). The highest-occupied molecular orbital (E_{HOMO}) and lowest-unoccupied molecular orbital (E_{LUMO}) energies were also examined. The following relationships [26–30] were used to compute the electronic band gap and Fermi level energy[23-29]:

$$E_{gap} = E_{HOMO} - E_{LUMO} \quad (1)$$

$$E_{Fl} = (E_{HOMO} - E_{LUMO}) /2 \quad (2)$$

We investigated the reactivity of these structures using the DFT approach and Koopmans theorem. The ionization potential (I_p), electron affinity (E_A), electronegativity (E_N), chemical hardness (H), chemical softness (S), and electrophilic (ω), which were computed using the following characteristics, are included in the description of the reactivity[7, 30]:

$$\mu = \left(\frac{\partial E}{\partial N}\right)_{V(\vec{r})} \tag{3}$$

$$H = \frac{1}{2}\left(\frac{\partial^2 E}{\partial N^2}\right)_{V(\vec{r})} \tag{4}$$

$$S = \frac{1}{2H} = \left(\frac{\partial^2 E}{\partial N^2}\right)_{V(\vec{r})} \tag{5}$$

$$\omega = \frac{\mu^2}{2H} \tag{6}$$

2. The electronic properties of the n-triangulene graphene nanoflakes (nT-GNFs)

First, the geometrical structures of all nT-GNFs are optimized using DFT calculations. After optimizing of all these structures of n-triangulene (where $n = 3 - 6$), we indicated that this method is very suitable to present all the above parameters due to these parameters being in agreement with previous theoretical and experimental studies [31, 32]. Then, we have used this method to calculate various electronic properties of all these structures.

We started by computing the electronic properties of 3T-GNFs, we detected that the 3T-GNFs has a semiconductor behavior with electronic band gap is 0.175 eV, as shown in Table 1. By computing the DOS, we detected that the shape of the DOS is changed (see Fig.1) and the electronic band gap is increased with replacing one C atom by Si impurity and it is increased more by altering the location of Si impurity, as represented in Table 1. Also, it is increased when the H atom is substituted by Si impurity compared with the pristine 3T-GNFs case due to the H atom has an atomic radius smaller than Si impurity , but it still has semiconductor behavior. The Fermi level is shifted up when the single C atom is exchanged with Si impurity, but it is shifted down when the single H atom is substituted with Si impurity and C_2 is swapped by Si_2 impurities, as represented in Table 1. Also, the electronic band gap is increased when the Si impurity is linked up to the 3T-GNFs, as shown in Fig.2. So, it is depending on the site of Si impurity. Fermi level is shifted up by using these locations of Si impurity.

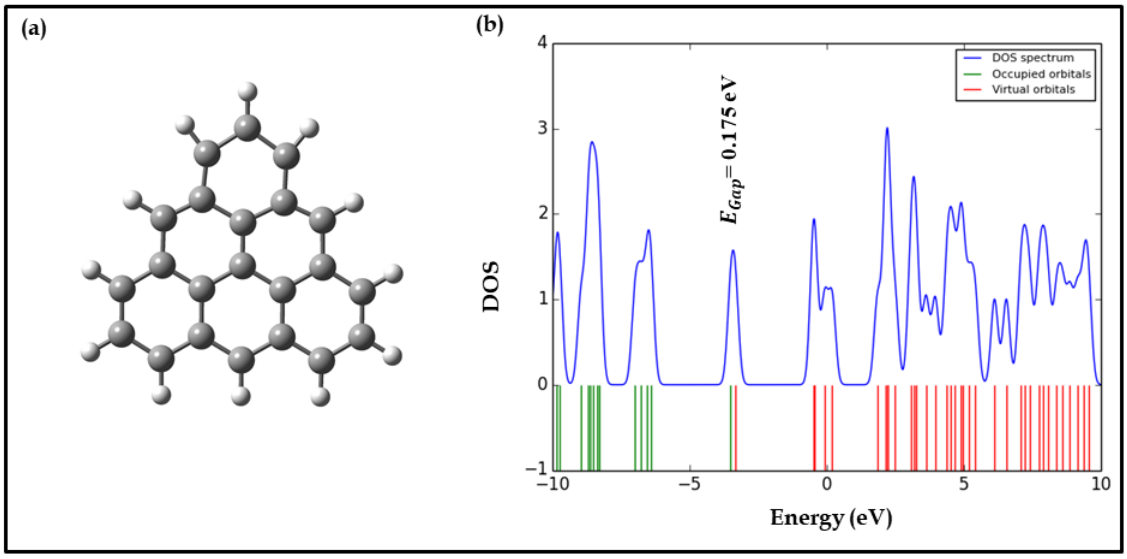

Figure -1 The electronic DOS of the pristine 3T-GNFs.

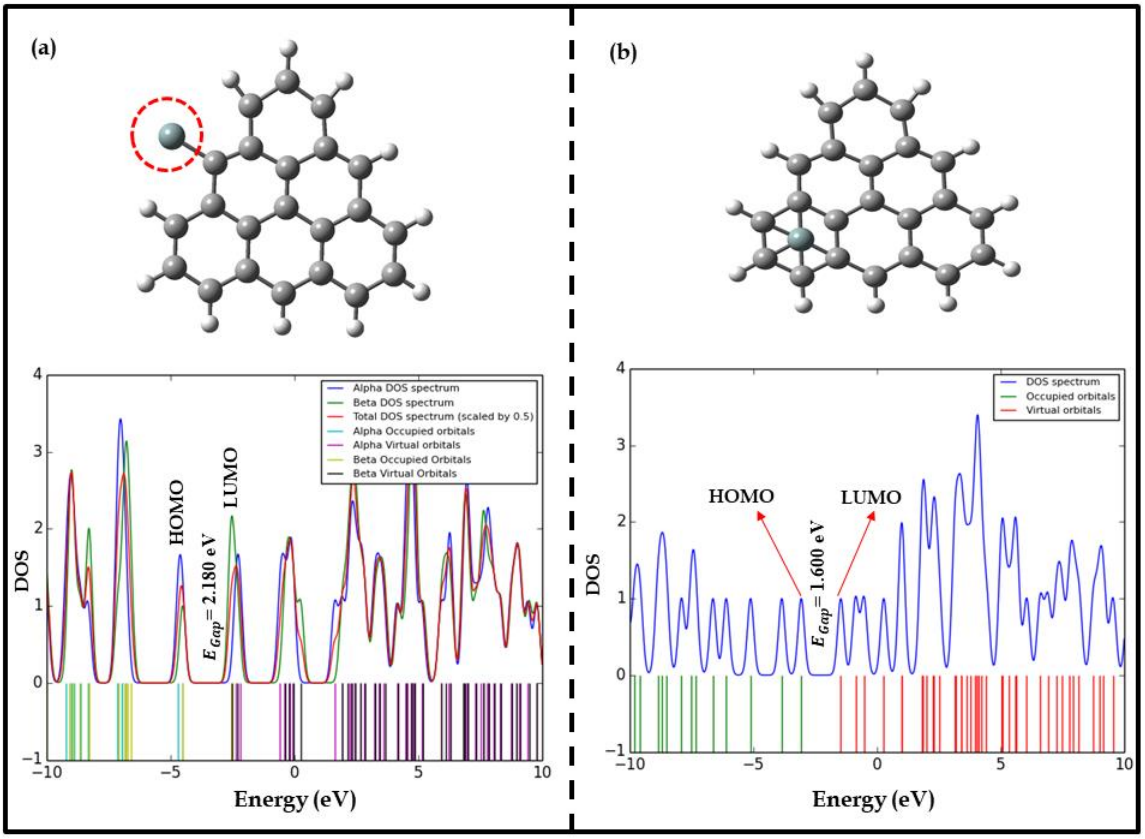

Figure - 2 The electronic DOS of the 3T-GNFs with various sites of Si impurity.

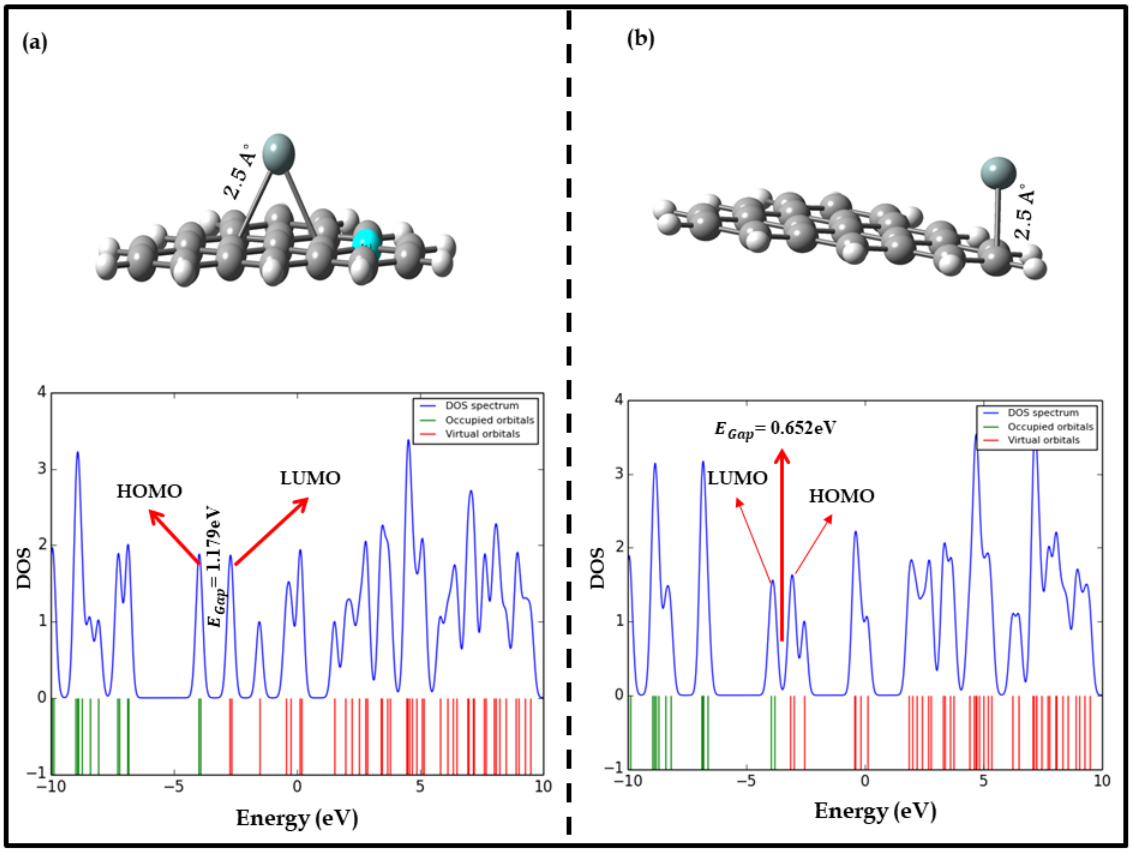

Figure -3 The electronic DOS of the Si impurity up to the 3T-GNFs .

For stability, the total energy of the 3T-GNFs is calculated. The results represented that the 3T-GNFs became more stable and lower reactive due to the total energy being increased by utilizing various concentrations of Si impurities in different locations. So, it is became more stable by replacing the single H atom with a single Si impurity, as shown in Table 1.

For 4T-GNFs, we detected that the electronic band gap is reduced by using P impurity in various locations, which are utilized in the 3T-GNFs, as presented in Figs.4-6 and summarized in Table 1. However, it is increased by replacing a single H atom with a single P impurity, as represented in Table 1. The results also displayed that the Fermi level is depended on the locations of P impurity. So, it is shifted down, as shown in Table 1. The total energy of the 4T-GNFs is increased, which led to making the structure became more stable and lower reactive, as displayed in Table 1.

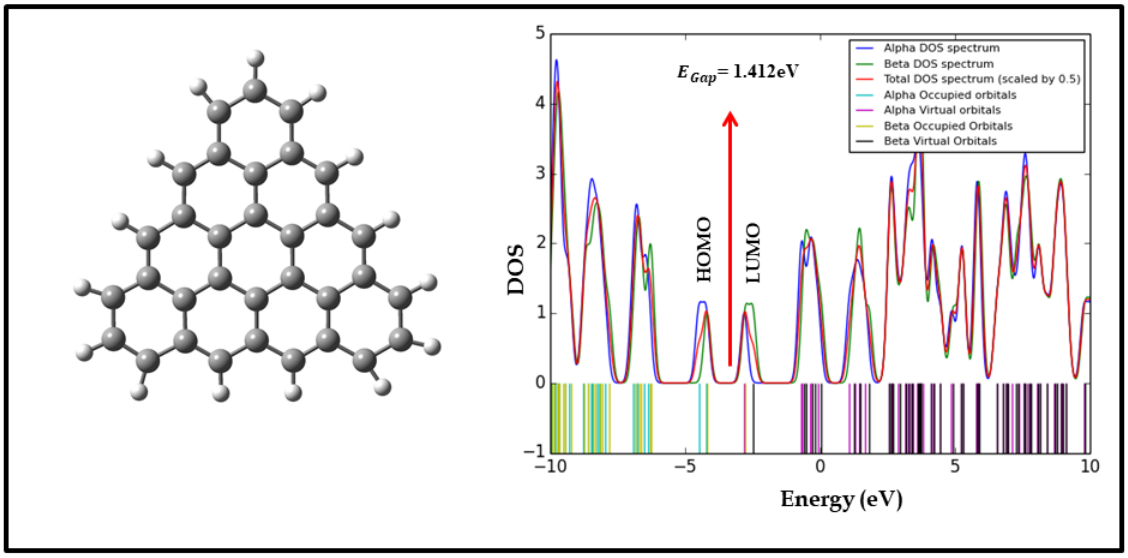

Figure -4 The electronic DOS of the pristine 4T-GNFs.

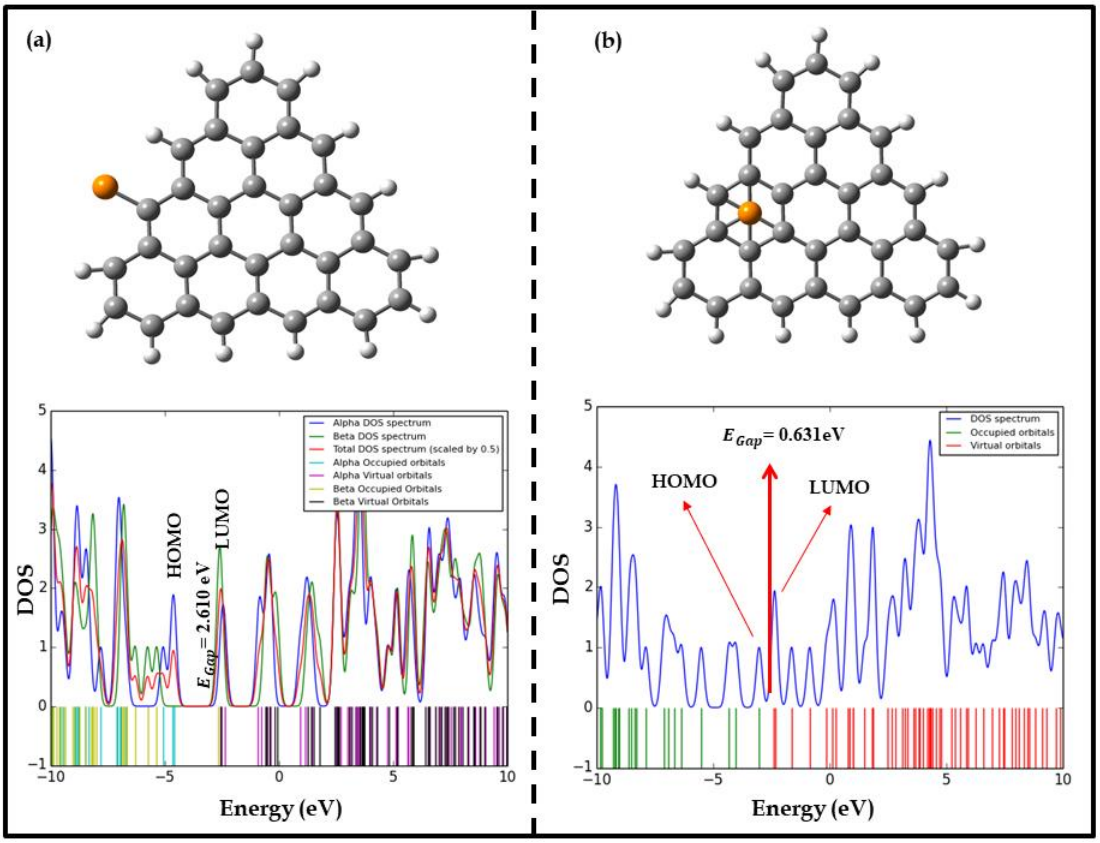

Figure -5 The electronic DOS of the 4T-GNFs with P impurity in different sites.

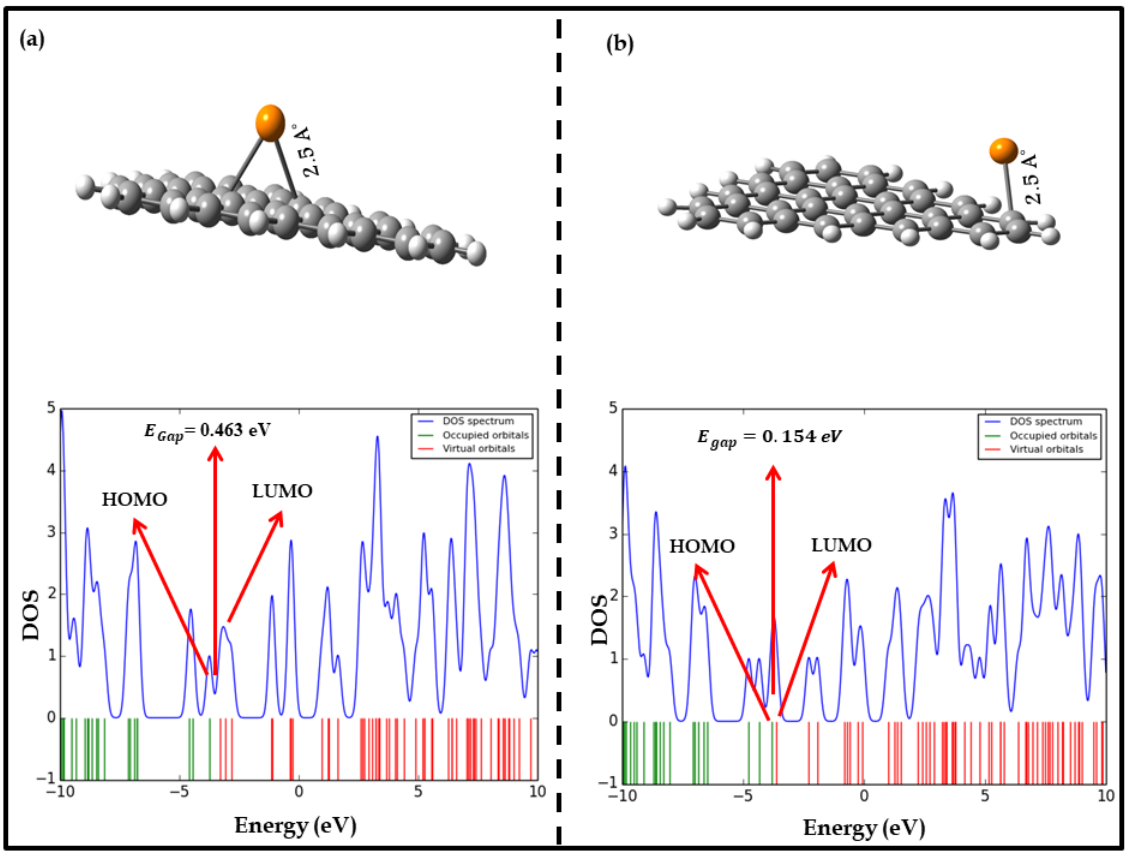

Figure -6 The electronic DOS of the P impurity up to the 4T-GNFs .

By increasing the number of C atoms to become (5T-GNFs), we detected that the electronic band gap is increased by using Ge impurity in different sites (in the same locations of impurities, which is used in various cases), as exhibited in Figs. 7-9 and summarized in Table 1. But, it is reduced when the single H atom is replaced with a single Ge impurity, as represented in Fig. 7(a). We also found out that these structures became more stable due to the total energy is increased with Ge impurity in different sites, as shown in Table 1.

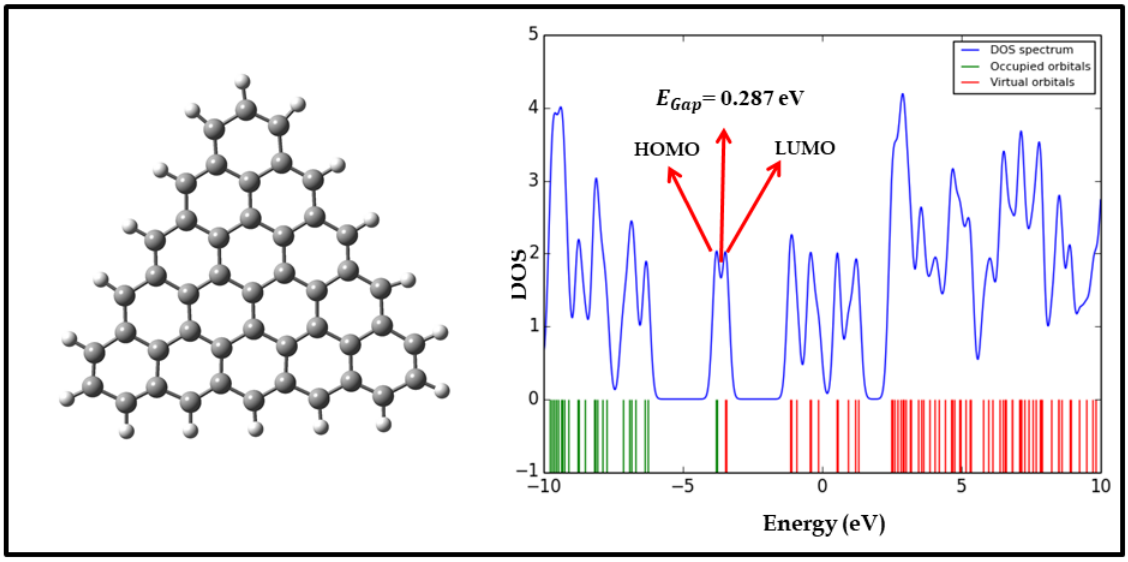

Figure -7 The electronic DOS of the pristine 5T-GNFs .

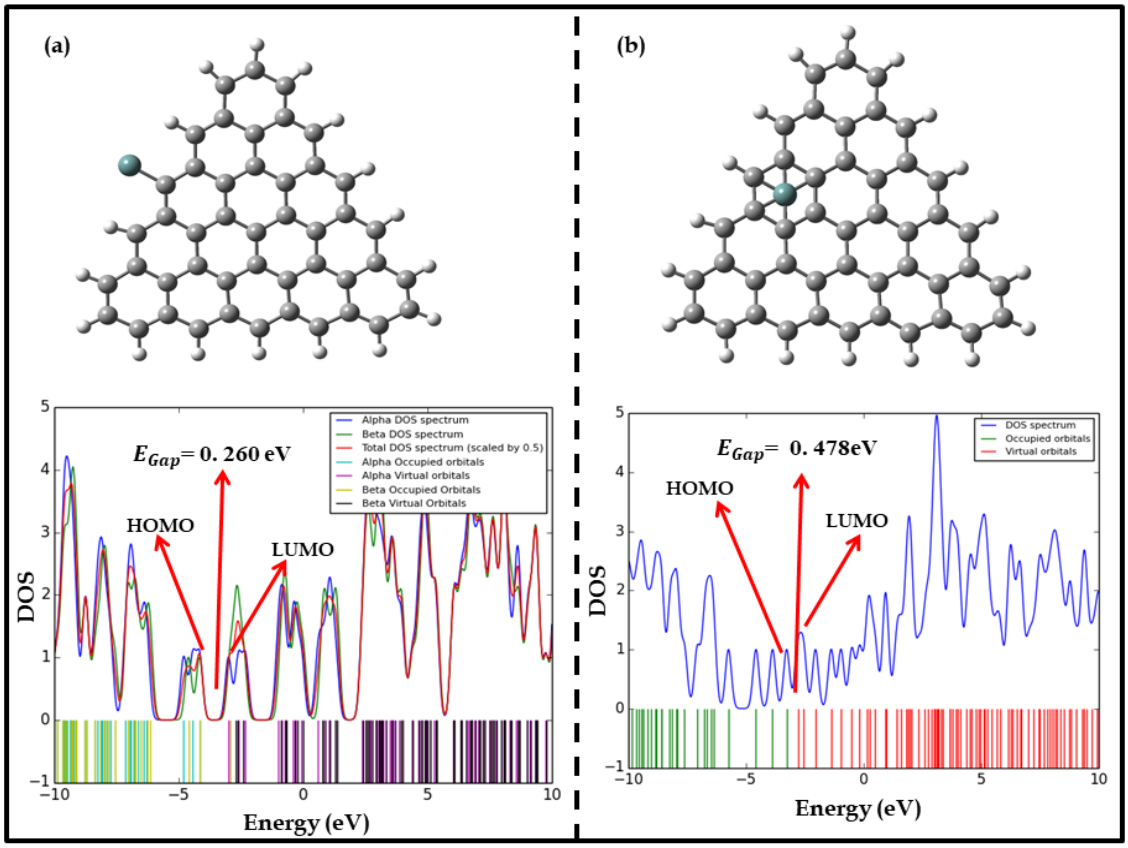

Figure -8 The electronic DOS of the Ge-doped 5T-GNFs in different sites.

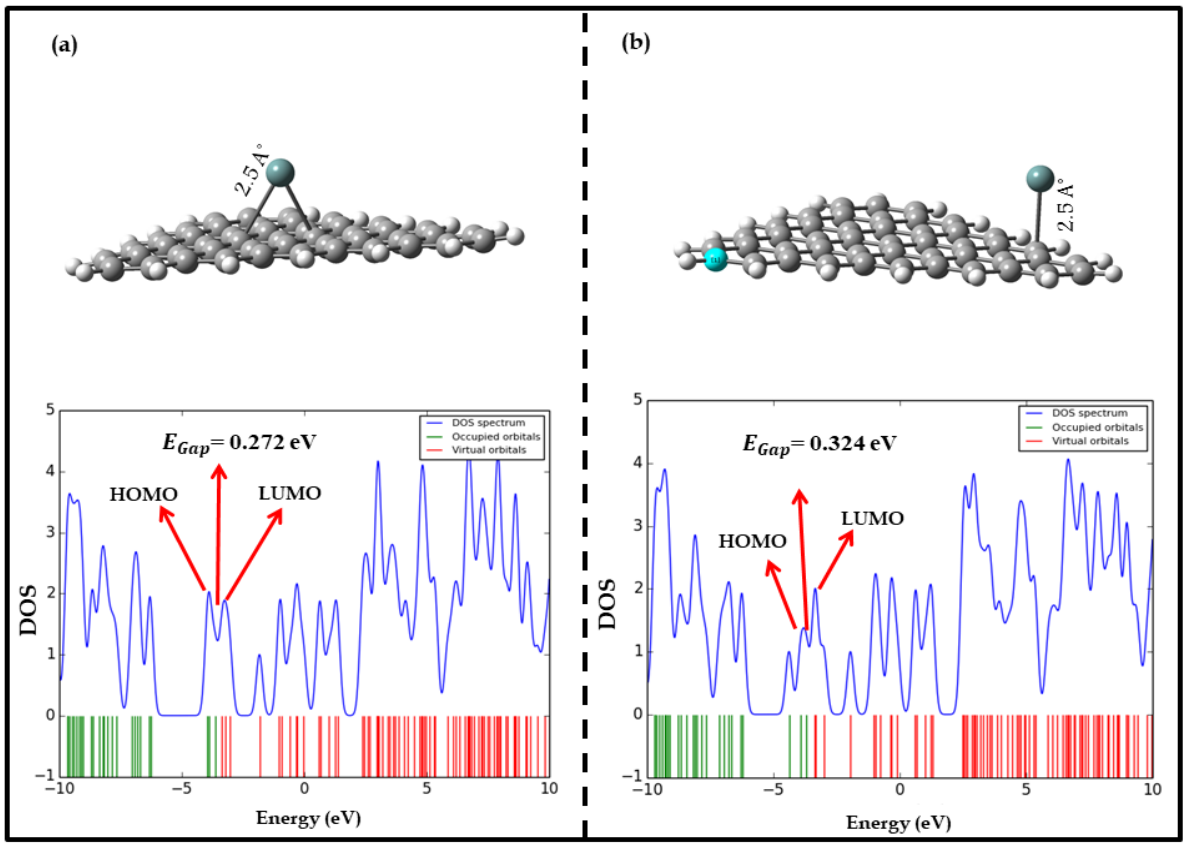

Figure -9 The electronic DOS of the Ge impurity up to the 5T-GNFs .

For 6T-GNFs, the results show that this structure has a semiconductor behavior. By utilizing As impurity in the same location, which is utilized in previous cases, we found out that this structure has the same behavior, but it is reduced by using As impurity in different sites, as displayed in Figs. 10-12 and summarized in Table 1. Moreover, this impurity affected on the stability of this structure. So, it is became more stable with this impurity, as demonstrated in Table 1.

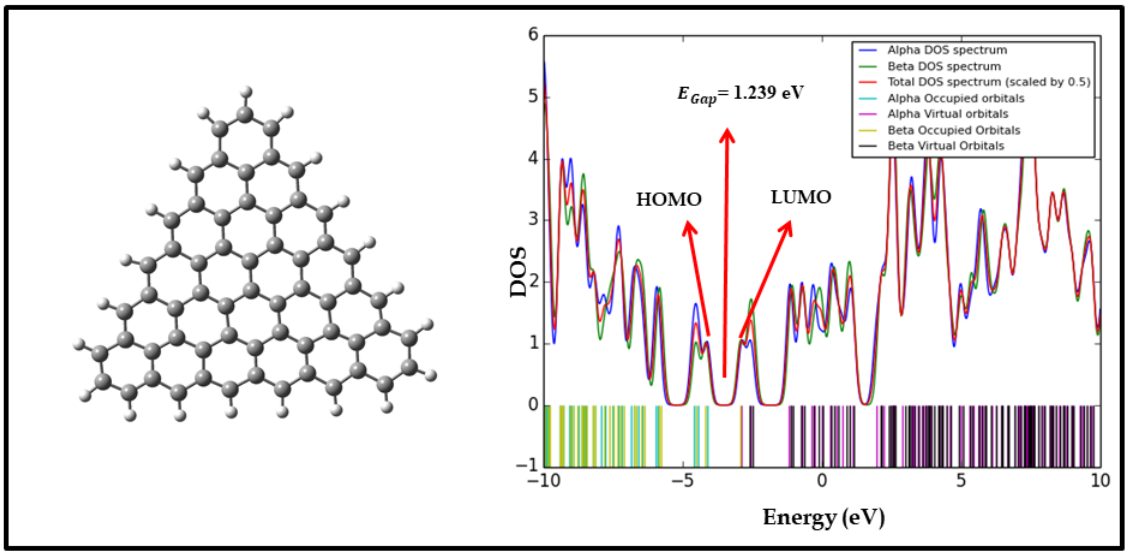

Figure -10 The electronic DOS of the pristine 6T-GNFs.

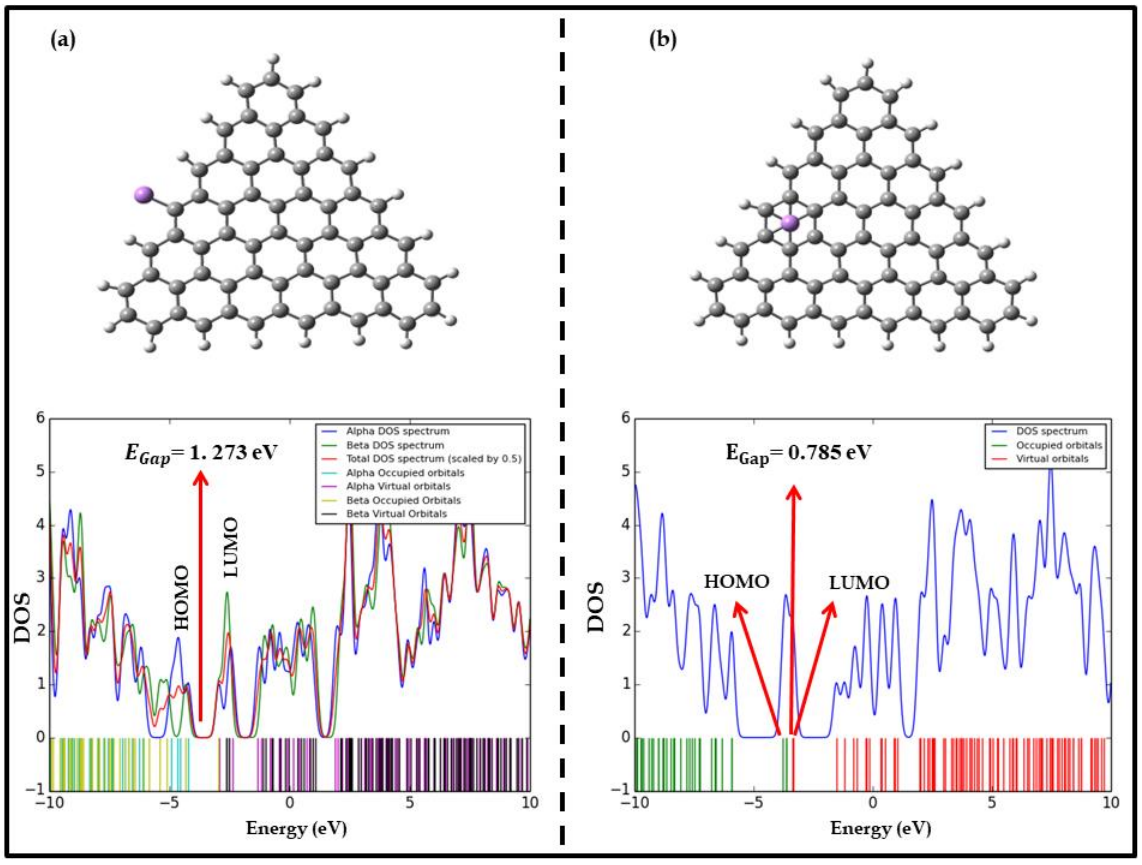

Figure -11 The electronic DOS of the 6T-GNFs with As impurity in different sites.

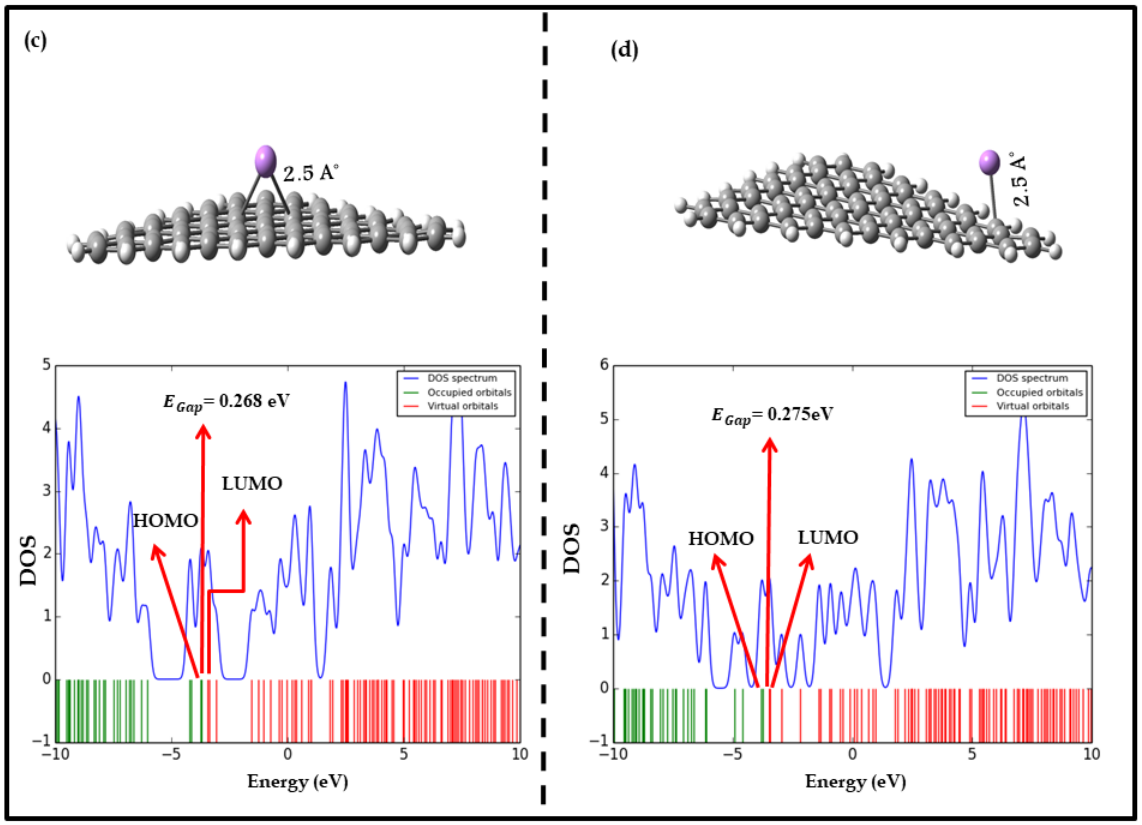

Figure -12 The electronic DOS of the impurity at different site in the 6T-GNFs.

Table 1- The electronic properties of the nT-GNFs with various impurities in various sites.

System	Type of dopants	E_T (eV)	α (Debye)	E_{HOMO} (eV)	E_{LUMO} (eV)	E_{gap} (eV)	E_{FL} (eV)
3T-GNFs	Pristine 3T-GNFS	-23001.585	4.465	-3.495	-3.320	0.175	-3.407
	Si-doped 3T-GNFs in site (1)	-30836.205	6.588	-3.059	-1.458	1.600	-2.258
	Si-doped 3T-GNFs in site (2) H	-30860.992	1.157	-4.527	-2.346	2.180	-3.436
	Si-doped up to the 3T-GNS in site (1)	-30875.493	1.411	-3.792	-3.139	0.652	-3.465
	Si-doped up to the 3T-GNS in site (2)	-30875.487	1.024	-3.920	-2.740	1.179	-3.330
4T-GNFs	Pristine 4T-GNFs	-34456.771	0.397	-4.221	-2.808	1.412	-3.514
	P-doped 4T-GNFs in site (1)	-43694.428	6.971	-3.022	-2.391	0.631	-4.217
	P-doped 4T-GNFs in site (2)	-43727.595	2.918	-4.574	-2.513	2.061	-3.543
	P-doped up to the 4T-GNFs in site (1)	-30876.303	1.699	-3.794	-3.640	0.154	-3.717
	P-doped up to the 4T-GNFs in site (2)	-43739.631	0.924	-3.738	-3.275	0.463	-3.506
5T-GNFs	Pristine 5T-GNFs	-47984.166	0.549	-3.771	-3.484	0.287	-3.627
	Ge-doped 5T-GNFs in site (1)	-104394.861	10.436	-3.266	-2.788	0.478	-3.027
	Ge-doped 5T-GNFs in site (2)	-103390.576	0.631	-3.726	-3.465	0.260	-3.595
	Ge-doped up to the 5T-GNFs in site (1)	-104442.922	1.146	-3.693	-3.369	0.324	-3.531
	Ge-doped up to the 5T-GNFs in site (2)	-104442.469	1.649	-3.641	-3.369	0.272	-3.505
6T-GNFs	Pristine 6T-GNFs	-63584.946	0.251	-4.104	-2.865	1.239	-3.484
	As-doped 6T-GNFs in site (1)	-124305.528	11.217	-4.511	-3.726	0.785	-4.119
	As-doped 6T-GNFs in site (2)	-124347.049	2.101	-4.206	-2.932	1.273	-3.569
	As-doped up to the 6T-GNFs in site (1)	-124361.136	1.459	-3.750	-3.475	0.275	-3.612
	As-doped up to the 6T-GNFs in site (2)	-124359.315	1.698	-3.700	-3.431	0.268	-3.565

By computing the ionization energy (I_P) and electron affinity (E_A) for 3T-GNFs, we detected that this structure requires a higher energy to donating/accepting an electron to become cation/anion due to there is a higher value of the I_P and lower of the E_A with Si impurity in various locations, except the site (1) has an opposite behaviour, as shown in Table 2. At the same time, the electronegative (E_N) and electrochemical hardness (H) are computed for 3T-GNFs. This structure needs a higher excitation energy to transfer electron due to there is a higher value of the

Table 2 : Some electronic properties of all structures with various impurities in different sites.

system	Type of dopants	I_P (eV)	E_A (eV)	E_N (eV)	H (eV)	S (eV)	μ (eV)	ω (eV)
3T-GNFs	Pristine 3T-GNFs	3.496	3.320	3.408	0.088	5.697	-3.408	0.510
	Si-doped 3T-GNFs in site (1)	3.059	1.459	2.259	0.800	0.625	-2.259	2.042
	Si-doped 3T-GNFs in site (2)	4.527	2.346	3.437	1.090	0.459	-3.437	6.440
	Si-doped up to the 3T-GNS in site (1)	3.792	3.140	3.466	0.326	1.532	-3.466	1.960
	Si-doped up to the 3T-GNS in site (2)	3.920	2.741	3.330	0.590	0.848	-3.330	3.271
4T-GNFs	Pristine 4T-GNFs	4.221	2.809	3.515	0.706	0.708	-3.515	4.363
	P-doped 4T-GNFs in site (1)	3.023	2.392	2.707	0.316	1.584	-2.707	1.157
	P-doped 4T-GNFs in site (2)	4.574	2.513	3.544	1.031	0.485	-3.544	6.471
	P-doped up to the 4T-GNFs in site (1)	3.794	3.640	3.717	0.077	6.481	-3.717	0.533
	P-doped up to the 4T-GNFs in site (2)	3.739	3.275	3.507	0.232	2.157	-3.507	1.426
5T-GNFs	Pristine 5T-GNFs	3.772	3.484	3.628	0.144	3.480	-3.628	0.946
	Ge-doped 5T-GNFs in site (1)	3.267	2.789	3.028	0.239	2.092	-3.028	1.096
	Ge-doped 5T-GNFs in site (2)	3.727	3.466	3.596	0.130	3.832	-3.596	0.844
	Ge-doped up to the 5T-GNFs in site (1)	3.693	3.369	3.531	0.162	3.086	-3.531	1.010
	Ge-doped up to the 5T-GNFs in site (2)	3.641	3.369	3.505	0.136	3.675	-3.505	0.836
6T-GNFs	Pristine 6T-GNFs	4.105	2.865	3.485	0.620	0.807	-3.485	3.763
	As-doped 6T-GNFs in site (1)	4.512	3.726	4.119	0.393	1.273	-4.119	3.332
	As-doped 6T-GNFs in site (2)	4.206	2.933	3.570	0.637	0.785	-3.570	4.056
	As-doped up to the 6T-GNFs in site (1)	3.751	3.475	3.613	0.138	3.631	-3.613	0.899
	As-doped up to the 6T-GNFs in site (2)	3.701	3.432	3.566	0.134	3.719	-3.566	0.855

H compared with pristine 3T-GNFs, as represented in Table 2. The results detected that the 4T-GNFs and 5T-GNFs have a reverse behaviour compared with 3T-GNFs, excepted the P-doped 4T-GNFs in site (2) has the same behaviour compared with 3T-GNFs. The 6T-GNFs has the same behaviour of the 3T-GNFs, excepted the As-doped up to the 6T-GNFs in site (1) and site (2) have the same behaviour of the 3T-GNFs, as represented in Table 2.

By computing the electronic softness (*S*) of all structures, we found out the S value depended on the locations of the impurity. So, it is decreased with all these impurities in all systems, which led to make these structures have a small separation between valence and conduction bands compared with pristine cases. However, the P-doped 4T-GNFs in site (1), P-doped up to the 4T-GNFs in sites (1 and 2), Ge-doped 5T-GNFs in site (2), Ge-doped up to the

5T-GNFs in site (2), As-doped 6T-GNFs in site (1), and As-doped up to the 6T-GNFs in sites (1and 2) have an opposite behaviour, as displayed in Table 2.

From the comparison of calculated the chemical potential (μ) and electrophilic index (ω) of all these structures, the large absolute value of the μ with the lower value of the ω (see Table 2) led to make these structures have a weak interact with other structures or molecular. But, the Si-doped 3T-GNFs in site (2), Pristine 4T-GNFs, P-doped 4T-GNFs in site (2), Pristine 6T-GNFs, and As-doped 6T-GNFs in site (2) have an opposed behaviour.

3. Conclusion

In this study, the electronic properties of the nT-GNFs with and without various concentrations of (Si, P, Ge, and As) impurities are exanimated via utilizing DFT method. We detected that the nT-GNFs is very sensitive to these impurities. So, the nT-GNFs became more stable and lower reactive due to the total energy is increased by utilizing these impurities. Also, the electronic band gap is altered, but it still has a semiconductor. We detected that some of these structures have weak interact with others structures. There are a higher energy required to donating/accepting an electron to become cation/anion. Briefly, the results exposed the electronic properties of all structures depended on the type and location of the impurity. At that time, we can use these impurities to improvement the electronic properties of the nT-GNFs.

References

[1] H. I. Sirikumara, E. Putz, M. Al-Abboodi, and T. Jayasekera, "Symmetry induced semimetal-semiconductor transition in doped graphene," *Scientific reports,* vol. 6, no. 1, p. 19115, 2016.

[2] G. Dresselhaus, M. S. Dresselhaus, and R. Saito, *Physical properties of carbon nanotubes*. World scientific, 1998.

[3] M. H. Al-Abboodi, F. N. Ajeel, and A. M. Khudhair, "Influence of oxygen impurities on the electronic properties of graphene nanoflakes," *Physica E: Low-dimensional Systems and Nanostructures,* vol. 88 ,pp. 1-5, 2017.

[4] M. H. Mohammed, "Controlling the electronic properties of the graphene nanoflakes by BN impurities," *Physica E: Low-dimensional Systems and Nanostructures,* vol. 95, pp. 86-93, 2018.

[5] F. Ajeel, A. Khudhair, M. Mohammed, and K. M. Mahdi, "DFT investigation of graphene nanoribbon as a potential nanobiosensor for tyrosine amino acid," *Russian Journal of Physical Chemistry A,* vol. 93, no. 4, pp. 778-785, 2019.

[6] M. H. Mohammed, "Electronic and thermoelectric properties of zigzag and armchair boron nitride nanotubes in the presence of C island," *Chinese Journal of Physics,* vol. 56, no. 4, pp. 1622-1632, 2018.

[7] M. H. Mohammed, A. S. Al-Asadi, and F. H. Hanoon, "Electronic structure and band gap engineering of bilayer graphene nanoflakes in the presence of nitrogen, boron and boron nitride impurities," *Superlattices and Microstructures,* vol. 129, pp. 14-19, 2019.

[8] M. H. Mohammed, A. S. Al-Asadi, and F. H. Hanoon, "Semi-metallic bilayer MS2 (M= W, Mo) induced by Boron, Carbon, and Nitrogen impurities," *Solid State Communications,* vol. 282, pp. 28-32, 2018.

[9] K. S. Novoselov *et al.*, "Two-dimensional gas of massless Dirac fermions in graphene," *nature*, vol. 438, no. 7065, pp. 197-200, 2005.

[10] A. K. Geim, "Graphene: status and prospects," *science*, vol. 324, no. 5934, pp. 1530-1534, 2009.

[11] C.-H. Park, L. Yang, Y.-W. Son, M. L. Cohen, and S. G. Louie, "Anisotropic behaviours of massless Dirac fermions in graphene under periodic potentials," *Nature Physics*, vol. 4, no. 3, pp. 213.2008 ,217-

[12] F. N. Ajeel, M. H. Mohammed, and A. M. Khudhair, "Energy bandgap engineering of graphene nanoribbon by doping phosphorous impurities to create nano-heterostructures: A DFT study," *Physica E: Low-dimensional Systems and Nanostructures*, vol ,105 .pp. 105-115, 2019.

[13] Y.-W. Son, M. L. Cohen, and S. G. Louie, "Erratum: energy gaps in graphene nanoribbons [Phys. Rev. Lett. 97, 216803 (2006)]," *Physical Review Letters*, vol. 98, no. 8, p. 089901, 2007.

[14] R. Majidi, "Electronic properties of T graphene-like C–BN sheets: a density functional theory study," *Physica E: Low-dimensional Systems and Nanostructures*, vol. 74, pp. 371-376, 2015.

[15] F. Nimr Ajeel, A. Mohsin Khuodhair, and S. Mahdi AbdulAlmohsin, "Improvement of the optoelectronic properties of organic molecules for nanoelectronics and solar cells applications: via DFT-B3LYP investigations," *Current Physical Chemistry*, vol. 7, no. 1, pp. 39-46, 2017.

[16] F. N. Ajeel, M. H. Mohammed, and A. M. Khudhair, "Tuning the electronic properties of the fullerene C 20 cage via silicon impurities," *Russian Journal of Physical Chemistry B*, vol. 11, no. 5, pp. 850-858, 2017.

[17] A. M. Khudhair, F. N. Ajeel, and M. H. Mohammed, "Engineering and design of simple models from dye-sensitive of solar cells and photovoltaic cells applications: Theoretical study," *Chemical Physics Letters*, 2018.

[18] F. N. Ajeel, A. M. Khudhair, and A. A. Mohammed, "Density functional theory investigation of the physical properties of dicyano pyridazine molecules," *International Journal of Science and Research*, vol. 4, no. 4, pp. 2334-2339, 2015.

[19] A. M. KHUODHAIR, F. N. AJEEL, and M. O. OLEIWI, "Density functional theory investigations for the electronic and vibrational properties of donor-acceptor system," *Journal of Applied Physical Science International*, vol. 6, no. 4, pp. 202-209, 2016.

[20] J. Beheshtian, A. A. Peyghan, Z. Bagheri, and M. B. Tabar, "Density-functional calculations of HCN adsorption on the pristine and Si-doped graphynes," *Structural Chemistry* ,vol. 25, no. 1, pp. 1-7, 2014.

[21] R. H. Hertwig and W. Koch, "On the parameterization of the local correlation functional. What is Becke-3-LYP?," *Chemical Physics Letters*, vol. 268, no. 5-6, pp. 345-351, 1997.

[22] M. W. Wong, "Vibrational frequency prediction using density functional theory," *Chemical Physics Letters*, vol. 256, no. 4-5, pp. 391-399, 1996.

[23] M. Hesabi and R. Behjatmanesh-Ardakani, "Interaction between anti-cancer drug hydroxycarbamide and boron nitride nanotube: a long-range corrected DFT study," *Computational and Theoretical Chemistry*, vol. 1117, pp. 61-80, 2017.

[24] F. N. Ajeel, M. H. Mohammed, and A. M. Khudhair, "SWCNT as a Model Nanosensor for Associated Petroleum Gas Molecules: Via DFT/B3LYP Investigations," *Russian Journal of Physical Chemistry B*, vol. 13, no. 1, pp. 196-204, 2019.

[25] F. N. Ajeel, "Engineering electronic structure of a fullerene C20 bowl with germanium impurities," *Chinese Journal of Physics*, vol. 55, no. 5, pp. 2134-2143, 2017.

[26] A. M. Khudhair, F. N .Ajeel, and M. H. Mohammed, "Theoretical (DFT and TDDFT) insights into the effect of polycyclic aromatic hydrocarbons on Monascus pigments and its implication as a photosensitizer for dye-sensitized solar cells," *Microelectronic Engineering*, vol. 212, pp-21 . .2019 ,26

[27] A. M. Khudhair, K. H. Bardan, A. Almusawe, and F. N. Ajeel, "Enhancement the electronic and optical properties for the dye Disperse Orange 13 and using in the solar cell device," in *IOP Conference Series: Materials Science and Engineering*, 2020, vol. 928, no. 7: IOP Publishing, p. 072031 .

[28] M. K. Hommod and L. F. Auqla, "Density Functional Theory Investigation For Ni6, Co5, Au12, Y5 and Ni6Li, Co5Li, Au12Li, Y5Na Interactions," *University of Thi-Qar Journal of Science*, vol. 9, no. 2 ,pp. 105-112, 2022.

[29] M. N. Mutier and L. F. Al-Badry, "Effect of Direct Coupling on Electronic Transport and Thermoelectric Properties of Single Pyrene Molecule," *University of Thi-Qar Journal of Science*, vol. 8, no. 2, pp. 94-99, 2021.

[30] F. N. Ajeel, M. H. Mohammed, and A. M. Khudhair, "SWCNT as a model nanosensor for associated petroleum gas molecules: via DFT/B3LYP investigations," *Russian Journal of Physical Chemistry B*, vol. 13, pp. 196-204, 2019.

[31] Q. Deng and J.-D. Chai, "Electronic properties of triangle-shaped graphene nanoflakes from TAO-DFT," *ACS omega*, vol. 4, no. 10, pp. 14202-14210, 2019.

[32] C. Terroso, F. de Souza, W. Paz, and F. N. N. Pansini, "Spin State Engineering of Triangulene Graphene Embedded in H-Bn Nanoflake".